Available online at www.sciencedirect.com
ScienceDirect
Trans. Nonferrous Met. Soc. China 22(2012) 2484−2490
Transactions of Nonferrous Metals Society of China
www.tnmsc.cn

Synthesis of nano-MoS_2/bentonite composite and its application for removal of organic dye

HU Kun-hong[1,2], ZHAO Di-fang[1], LIU Jun-sheng[1]

1. Department of Chemical and Materials Engineering, Hefei University, Hefei 230022, China;
2. Postdoctoral Working Station of Materials Science and Engineering, Hefei University of Technology, Hefei 230009, China

Received 9 July 2012; accepted 6 August 2012

Abstract: A nano-MoS_2/bentonite composite was synthesized by calcinating MoS_3 deposited on bentonite in H_2. The obtained composite was characterized using thermogravimetric analysis, X-ray diffractometer, scanning electron microscope and transmission electron microscope. The results show that nano-MoS_2 particles are distributed on the surface of bentonite and form layered structures with layer distance of about 0.64 nm. The composite presents an excellent performance for the removal of methyl orange. Some operation conditions affect the removal efficiency of methyl orange, such as dosage of composite, initial concentration of methyl orange, temperature and pH value. However, light source does not influence the removal efficiency. The removal mechanism is attributed to the adsorption of methyl orange on the nano-MoS_2/bentonite composite. The adsorption of methyl orange on the composite is in accordance with the pseudo-second-order kinetic model.

Key words: molybdenum disulfide; bentonite; nanoparticles; photocatalysis; adsorption; organic dye

1 Introduction

Molybdenum disulfide (MoS_2) is a typical layered compound with weak van der Waals gap and reveals excellent properties in catalysis and lubrication. As for the catalytic properties, MoS_2 has been vastly used as catalysts to remove S and N from crude oils [1−3]. Nanosized MoS_2 (nano-MoS_2) usually has better properties than bulk MoS_2, thus attracting so much attention [4−8]. Some chemical methods have been reported to synthesize nano-MoS_2 particles in various shapes [9−12]. The catalytic performance of nano-MoS_2 has also been investigated [13,14]. When the size of MoS_2 is decreased to nanoscale, Mo edge-site atoms become chemically active without the protection from the inert basal planes of MoS_2. Correspondingly, the band gap of nano-MoS_2 becomes low enough to absorb the solar spectrum, resulting in potential applications in photo catalysts [15−17].

Natural minerals are often used as supporters in photo catalysts such as zeolite and attapulgite [18,19]. In previous study, a nano-MoS_2 composite was synthesized by depositing platelet-like MoS_2 nanoparticles on a kaolin supporter [20]. The composite showed very high capability for the removal of methyl orange from aqueous solutions and the removal mechanism was attributed to the photo catalytic activity of nano-MoS_2. In the present work, the synthesis of a MoS_2/bentonite composite was investigated. The composite revealed very high activity for the removal of methyl orange. However, the removal mechanism was mainly attributed to the adsorption of methyl orange on the nano-MoS_2/bentonite composite.

2 Experimental

2.1 Synthesis of nano-Mos_2/bentonite composite

All the chemical reagents used were of analytical grade. 0.6 g $Na_2MoO_4·2H_2O$ and 3.4 g $Na_2S·9H_2O$ were added to 100 mL de-ionized water with 10 mL alcohol dispersant. Bentonite was dispersed in the above solution with stirring. 8 mL 12 mol/L HCl was then added to the obtained suspension. The precipitation reaction

Foundation item: Project (2011M500110) supported by the Postdoctoral Science Foundation of China; Project (50905054) supported by the National Natural Science Foundation of China; Project (12RC03) supported by Hefei University, China
Corresponding author: HU Kun-hong; Tel: +86-13966745693; E-mail: hukunhong@gmail.com
DOI: 10.1016/S1003-6326(11)61489-1

immediately began between Na_2MoO_4 and Na_2S, leading to a brown precursor. After being dried at 105 °C, the as-synthesized precursor was calcinated at 450 °C under a H_2 flow for 30 min to produce the desired nano-MoS_2/bentonite composites. A pure nano-MoS_2 sample was also synthesized by the similar method.

2.2 Characterization

The calcination of the brown precursor was studied on a Netzsch model TG209 thermo gravimetric analyzer (TGA). The nano-MoS_2/bentonite was characterized using a Rigaku D/Max−2500V X-ray diffractometer (XRD), a Philips XT30 ESEM-TMP scanning electron microscope (SEM), a Hitachi H−800 transmission electron microscopy (TEM) and a JEOL 2010 high-resolution transmission electron microscope (HRTEM).

2.3 Removal of methyl orange

The removal efficiency of methyl orange on the nano-MoS_2/bentonite composites was evaluated using the absorbance of methyl orange solution at a wavelength of 464 nm. The methyl orange solution with the composites was stirred in a quartz glass reactor. The absorbance (A) of methyl orange solution was measured every 15 min on a 721 spectrophotometer (Shanghai Precision & Scientific Instrument Company, China) after centrifugation of 3000 r/min for 5 min. The removal efficiency E was calculated from the formula: $E=(A_0-A)/A_0$, where A_0 is the initial absorbance. As a comparison, the pure nano-MoS_2 and bentonite were also studied.

3 Results and discussion

3.1 Synthesis of nano-MoS_2/bentonite

Bentonite is not easy to dissolve in the cold HCl solution. However, there exists a chemical corrosion on the surface of bentonite when high concentration hydrochloric acid is used. The weak chemical corrosion activates the insoluble mineral surfaces and provides nucleation sites for the deposition of MoS_3 [20]. Thus, the precursor (MoS_3) easily deposits on bentonite to form a composite according to the following reaction:

$$3S^{2-}+MoO_4^{2-}+8H^{+}+\text{Bentonite}\rightarrow \text{MoS}_3/\text{Bentonite}\downarrow+4H_2O \quad (1)$$

The calcination of the MoS_3/bentonite precursor was studied using TGA, and the results are shown in Fig. 1. As shown in this figure, the initial decomposition temperature of MoS_3/bentonite is about 395 °C. The decomposition of MoS_3/bentonite is completed at 450 °C. When the temperature exceeds 450 °C, the obvious decomposition of bentonite is observed. This indicates that higher temperatures easily lead to structural changes of bentonite. Thus, 450 °C was used in this work. Moreover, the bentonite is still slightly decomposed even at 450 °C according to the TGA curve. To avoid the adverse decomposition, a short treatment time of 30 min was selected. The calcination reaction is shown as follows:

$$\text{MoS}_3/\text{bentonite} + H_2 \xrightarrow{450\ ^\circ\text{C for 30 min}} \text{nano-MoS}_2/\text{bentonite} + H_2S \quad (2)$$

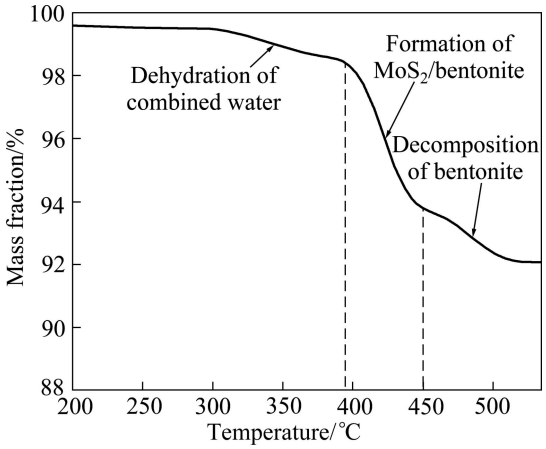

Fig. 1 TGA curve of MoS_3/bentonite precursor

3.2 Characterization of nano-MoS_2/bentonite

Figure 2 shows the XRD pattern of the resultant in reaction (2). The main diffraction peaks in the XRD pattern are indexed to bentonite (JCPDS No. 03-0019) or nano-MoS_2 [21]. Moreover, minor peaks in the XRD pattern could not be indexed, which are ascribed to the decomposing resultants of bentonite such as metal oxides. The findings confirm that the MoS_2/bentonite is successfully prepared, accompanied by a small quantity of impurities.

The micrographs of the nano-MoS_2/bentonite composite are shown in Fig. 3. The composite is

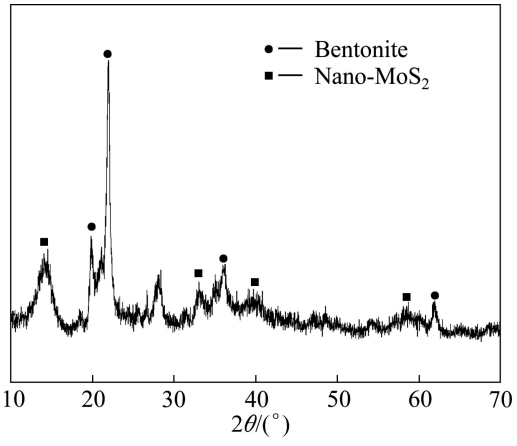

Fig. 2 XRD pattern of nano-MoS_2/bentonite composite

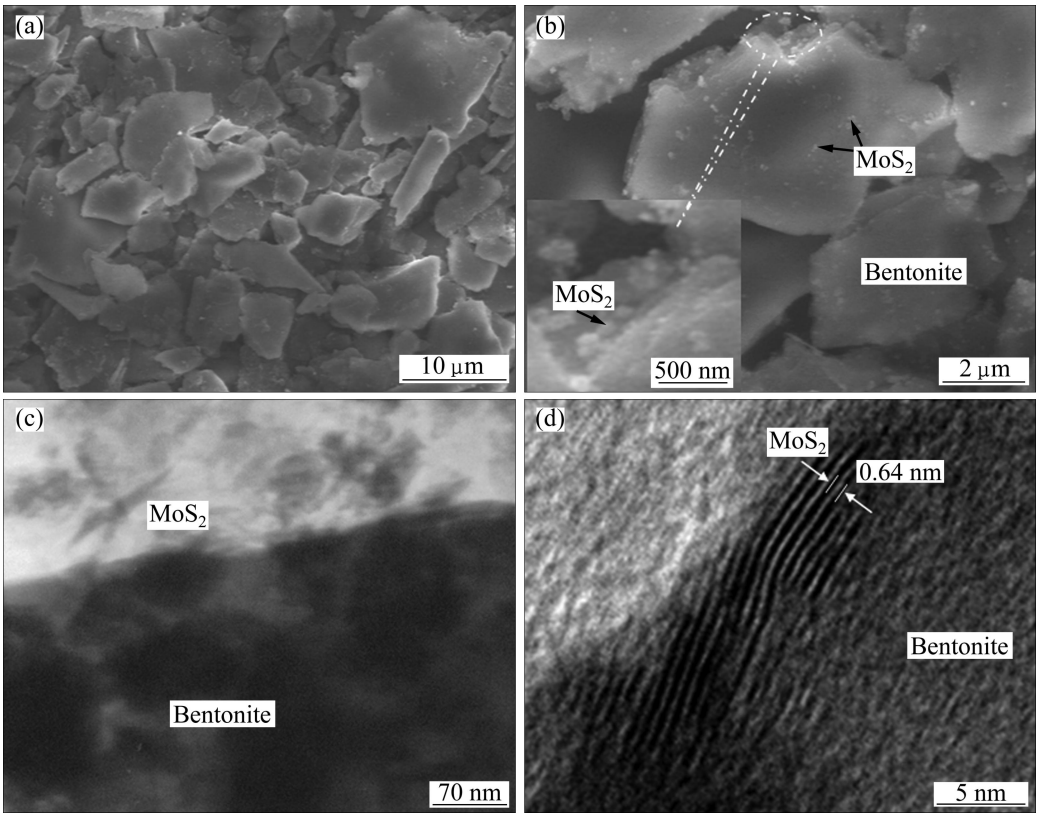

Fig. 3 Micrographs of nano-MoS_2/bentonite composite: (a, b) SEM; (c) TEM; (d) HRTEM

composed of bulk particles of 5−10 μm in size and nano-MoS_2 particles with very small sizes are distributed on the surface of bentonite (Figs. 3(a) and (b)). The TEM image in Fig. 3(c) also confirms that the nano-MoS_2 is deposited on the surface of bentonite. As shown in the high-resolution TEM (HRTEM) image (Fig. 3(d)), the nano-MoS_2 on bentonite forms layered structure with layer distance of about 0.64 nm, which is close to that of the typical 2H-MoS_2 (0.615 nm).

3.3 Removal of methyl orange

Figure 4 shows the effect of mass ratio of MoS_2 to bentonite on the removal efficiency of methyl orange from aqueous solutions. As shown in the figure, 0.075 g pure nano-MoS_2 leads to a relatively low removal efficiency of methyl orange (20 mg/L). The composite with mass ratio of MoS_2 to bentonite 1:4 results in a lower removal efficiency as compared to the pure nano-MoS_2. Similar removal efficiency of methyl orange is observed at mass ratio of 1:1 and the pure nano-MoS_2. However, the two nano-MoS_2/bentonite composites with mass ratio of 2:1 and 4:1 reveal very high activity in the removal of methyl orange. The figure also indicates that the activity is improved when the content of nano-MoS_2 in the composite is increased.

The nano-MoS_2/bentonite composite with mass ratio of 4:1 was selected as a sample to study the effect

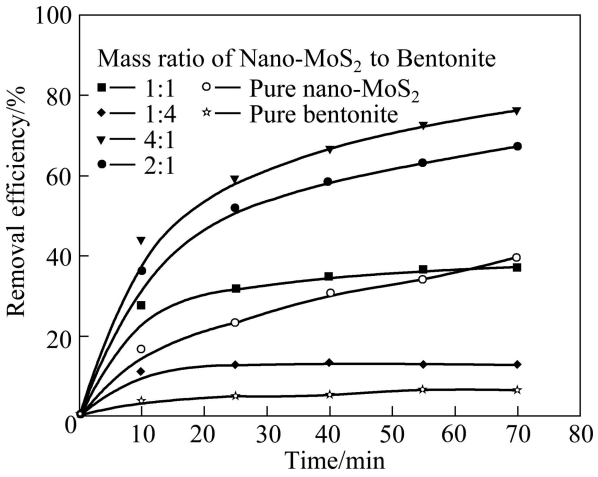

Fig. 4 Effect of mass ratio of MoS_2 to bentonite on removal of methyl orange from aqueous solutions

of operation conditions on the removal efficiency of methyl orange from water, and the results are shown in Fig. 5. As shown in Fig. 5(a), the removal efficiency within 70 min attains a satisfactory level (about 88%) when the dosage of composite is increased to 0.1 g in 150 mL 20 mg/L methyl orange solution. However, the dosage of 0.05 g is not enough to treat 150 mL methyl orange solution within 70 min. Figure 5(b) indicates that the initial concentration remarkably affects the removal efficiency of methyl orange by the composite. The

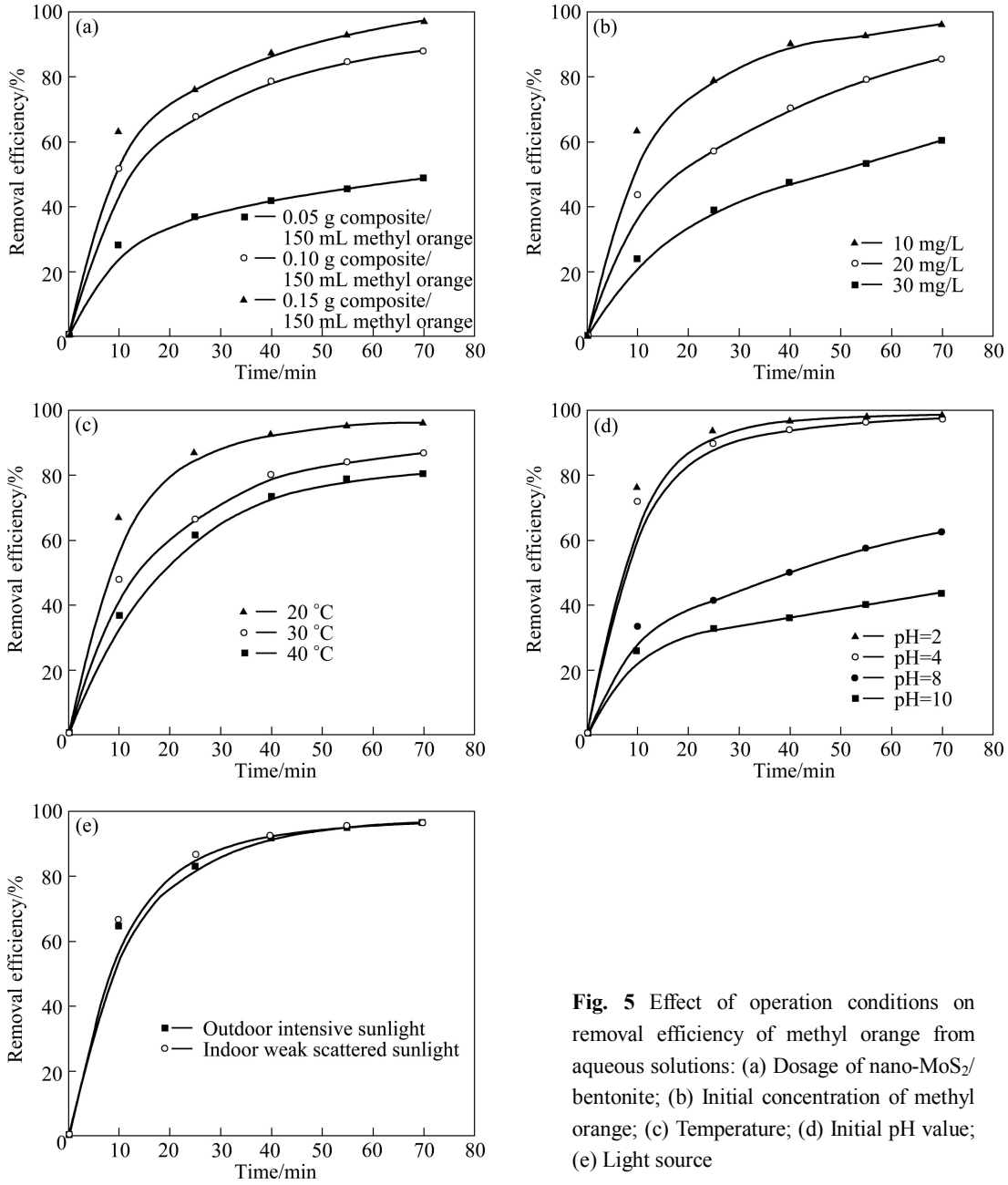

Fig. 5 Effect of operation conditions on removal efficiency of methyl orange from aqueous solutions: (a) Dosage of nano-MoS_2/bentonite; (b) Initial concentration of methyl orange; (c) Temperature; (d) Initial pH value; (e) Light source

removal efficiency decreases with increasing the initial concentration. The removal efficiency is satisfactory only when the initial concentration is less than 20 mg/L with the composite of 0.075 g. The removal efficiency of methyl is also influenced by temperature and pH value (Figs. 5(c) and (d)). The composite is more effective on the removal efficiency of methyl orange at a relatively low temperature. The removal efficiency of methyl orange is high in acidic solutions but low under alkaline conditions. The results are consistent with those reported in Refs. [20,21]. However, light source has no effect on the removal efficiency of methyl orange (Fig. 5(e)).

3.4 Regeneration of nano-MoS_2/bentonite

Figure 6 shows the influence of regeneration methods of the nano-MoS_2/bentonite composite on the removal efficiency of methyl orange. The nano-MoS_2/bentonite composite regenerated via filtration presents very low removal activities after one repeated use. However, the removal activity of nano-MoS_2/bentonite is completely recovered after calcination at 450 °C in H_2.

3.5 Removal mechanism of methyl orange

The platelet-like nano-MoS_2 can remove organic chemicals from wastewater because of its excellent photocatalytic performance under visible light [20]. The photocatalytic mechanism of nano-MoS_2 is attributed to the formation of hydroxyl radicals (·OH) from the adsorbed water by valence band holes under visible light [16].

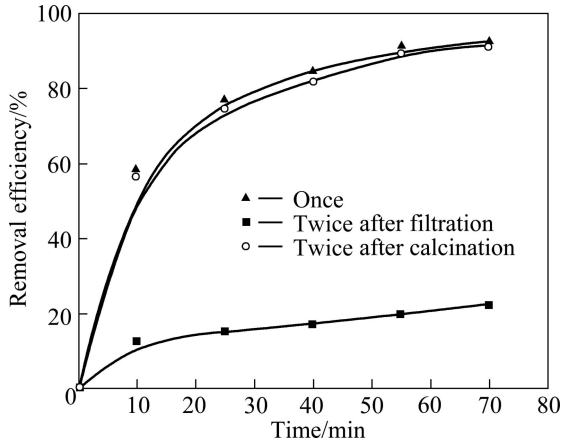

Fig. 6 Influence of regeneration methods of nano-MoS_2/bentonite composite on removal efficiency of methyl orange from aqueous solutions

$$MoS_2\cdots H_2O+h\nu \longrightarrow MoS_2+\cdot OH+H^+ \quad (3)$$

Moreover, the adsorption of the nano-MoS_2 is also a factor for the removal of organic compounds. The temperature has minor effects on the reaction rate for a photocatalytic reaction. However, for an adsorption process, the increasing temperature can generally decrease the adsorption amount of organic chemicals on the adsorbent, which is confirmed by the result in Fig. 5(c). Moreover, the light source can remarkably affect the catalytic degradation reaction of methyl orange [22]. However, as shown in Fig. 5(e), the light source has no effect on the removal efficiency of methyl orange. According to these mentioned above, the removal mechanism is mainly attributed to the adsorption of methyl orange on the nano-MoS_2/bentonite composite.

Generally, the adsorption ratio can be magnified by increasing dosage of the adsorbent and decreasing initial concentration of adsorbed substances. Thus, the removal efficiency of methyl orange is increased with increasing dosage of nano-MoS_2/bentonite and decreasing initial concentration of methyl orange (Figs. 5(a) and (b)). Methyl orange exhibits low adsorption level under alkaline conditions, whereas acidic solution remarkably improves the removal efficiency of methyl orange (Fig. 5(d)). Methyl orange may present two molecular structures, i.e., quinoid methyl orange under acidic condition and azo methyl orange under alkaline condition. The easy adsorption of methyl orange under acidic condition confirms that the nano-MoS_2/bentonite composite has a higher activity for the adsorption of the quinoid methyl orange.

3.6 Adsorption kinetics

The adsorption of methyl orange on the nano-MoS_2/bentonite composite is demonstrated using the pseudo-first-order and pseudo-second-order models as follows [23,24]:

Pseudo-first-order equation

$$\lg(q_e - q_t) = \lg q_e - \frac{k_1}{2.303}t \quad (4)$$

Pseudo-second-order equation

$$\frac{t}{q_t} = \frac{1}{k_2 q_e^2} + \frac{t}{q_e} \quad (5)$$

where q_t is the adsorption amount; q_e is the equilibrium adsorption amount; t is the time; k_1 and k_2 are the adsorption rate constants.

Figure 7(a) provides the results of pseudo-first-order model. As shown in the figure, the linear fitting degree (R^2) is only 0.907 in the pseudo-first-order linear fitting. The equilibrium adsorption amount (q_e) is 17.25 mg/g, which is deviated from the experimental value (44.56 mg/g). These indicate that the pseudo-first-order model cannot be used to explain the removal of methyl orange on the composite. However, the pseudo-second-order fitting is well consistent with the experimental results (Fig. 7(b)). The equilibrium adsorption amount is 46.84 mg/g, calculated according to the pseudo-second-order fitting curve, which is very

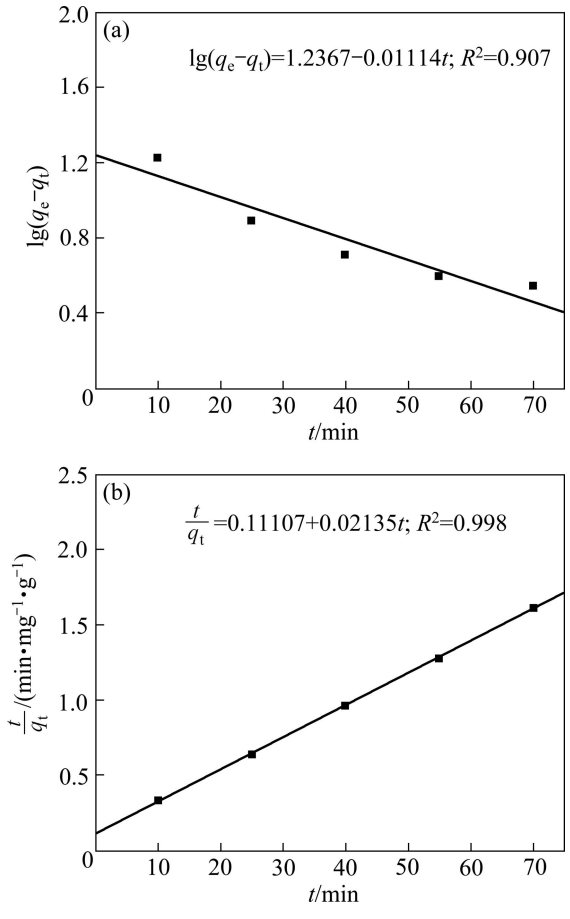

Fig. 7 Adsorption kinetics of methyl orange on nano-MoS_2/bentonite composite at 20 °C: (a) Pseudo-first-order linear fitting; (b) Pseudo-second-order linear fitting

close to the experimental value. Moreover, the R^2 (0.998) is also satisfactory in the pseudo-second-order fitting. Thus, the adsorption of methyl orange on the nano-MoS_2/bentonite composite may be demonstrated using the pseudo-second-order model. This also indicates that the removal of methyl orange results from its chemical adsorption on the nano-MoS_2/bentonite composite. The adsorption equation at 20 °C may be described as:

$$\frac{t}{q_t} = 0.11107 + 0.02135t \quad (6)$$

4 Conclusions

1) The nano-MoS_2/bentonite composite can be synthesized by depositing nano-MoS_2 on the acidified surface of bentonite. The as-prepared composite has an excellent performance for the removal of the organic dye.

2) Some operation conditions obviously affect the performance of composite including the mass ratio of nano-MoS_2 to bentonite, initial concentration of methyl orange, temperature and pH value. However, the light source does not influence the removal efficiency of methyl orange from aqueous solution.

3) The removal mechanism is mainly attributed to the adsorption of methyl orange on the nano-MoS_2/bentonite composite. The adsorption of methyl orange is in accordance with the pseudo-second-order kinetic model.

References

[1] KOCHUBEY D I, ROGOV V A, BABENKO V P. Thiophene hydrodesulfurization activity of MoS_2/Al_2O_3 catalysts prepared via exfoliation: The effect of cobalt [J]. React Kinet Catal Lett, 2004, 83: 181−186.

[2] ALONSO G, BERHAULT G, AGUILAR A, COLLINS V, ORNELAS C, FUENTES S, CHIANELLI R R. Characterisation and HDS activity of mesoporous MoS_2 catalysts prepared by in situ activation of tetraalkylammonium thiomolybdates [J]. J Catal, 2002, 208: 359−369.

[3] VALYON J, HALL W K. The chemisorption of O_2 and NO on reduced and sulfide molybdena-alumina catalysts [J]. J Catal, 1983, 84: 216−228.

[4] MENG Qing-juan, ZHANG Sheng-mao, YU Lai-gui, WU Zhi-shen, ZHANG Zhi-jun. Preparation of nanoscale water-dispersible molybdenum disulfide and evaluation of its tribological behavior [J]. Tribology, 2011, 31(2): 144−149. (in Chinese)

[5] FELDMAN Y, WASSERMAN E, SROLOVITZ D J, TENNE R. High rate, gas phase growth of MoS_2 nested inorganic fullerenes and nanotubes [J]. Science, 1995, 267: 222−225.

[6] NATH M, GOVINDARAJ A, RAO C N R. Simple synthesis of MoS_2 and WS_2 nanotubes [J]. Adv Mater, 2001, 13: 283−286.

[7] LAVAYEN V, MIRABAL N, O'DWYER C, SANTA ANA M A, BENAVENTE E, SOTOMAYOR TORRES C M, GONZÁLEZ G. The formation of nanotubes and nanocoils of molybdenum disulphide [J]. Appl Surf Sci, 2007, 253: 5185−5190.

[8] CIZAIRE L, VACHER B, MOGNE T L, MARTIN J M, RAPOPORT L, MARGOLIN A, TENNE R. Mechanisms of ultra-low friction by hollow inorganic fullerene-like MoS_2 nanoparticles [J]. Surf Coat Technol, 2002, 160: 282−287.

[9] LIU S, ZHANG X, SHAO H, XU J, CHEN F, FENG Y. Preparation of MoS_2 nanofibers by electrospinning [J]. Mater Lett, 2012, 73: 223−225.

[10] LIN H, CHEN X, LI H, YANG M, QI Y. Hydrothermal synthesis and characterisation of MoS_2 nanorods [J]. Mater Lett, 2010, 64: 1748−1750.

[11] RAPOPORT L, MOSHKOVICH A, PERFILYEV V, LAIKHTMAN A, LAPSKER I, YADGAROV L, ROSENTSVEIG R, TENNE R. High lubricity of re-doped fullerene-like MoS_2 nanoparticles [J]. Tribol Lett, 2012, 45: 257−264.

[12] CHEN Xiao-ya, LI Hong-ling, WANG Shi-ming, YANG Min, QI Yan-xing. A simple biomolecule-assisted hydrothermal synthesis of flower-like MoS_2 microspheres [J]. New Chemical Material, 2011, 39(5): 92−94. (in Chinese)

[13] THURSTON T R, WILCOXON J P. Photooxidation of organic chemicals catalyzed by nanoscale MoS_2 [J]. J Phys Chem B, 1999, 103: 11−17.

[14] WILCOXON J P, NEWCOMER P P, SAMARA G A. Synthesis and optical properties of MoS_2 and isomorphous nanoclusters in the quantum confinement regime [J]. J Appl Phys, 1997, 81: 7934−7944.

[15] POURABBAS B, JAMSHIDI B. Preparation of MoS_2 nanoparticles by a modified hydrothermal method and the photo-catalytic activity of MoS_2/TiO_2 hybrids in photo-oxidation of phenol [J]. Chem Eng J, 2008, 138: 55−62.

[16] HO W K, YU J C, LIN J, YU J G, LI P S. Preparation and photocatalytic behavior of MoS_2 and WS_2 nanocluster sensitized TiO_2 [J]. Langmuir, 2004, 20: 5865−5869.

[17] KANDA S, AKITA T, FUJISHIMA M, TADA H. Facile synthesis and catalytic activity of MoS_2/TiO_2 by a photodeposition-based technique and its oxidized derivative MoO_3/TiO_2 with a unique photochromism [J]. J Colloid Interface Sci, 2011, 354: 607−610.

[18] HUANG M, XU C, WU Z, HUANG Y, LIN J, WU J. Photocatalytic discolorization of methyl orange solution by Pt modified TiO_2 loaded on natural zeolite [J]. Dyes Pigm, 2008, 77: 327−334.

[19] ZHAO Xiao-bing, JIN Chao, ZHANG Yue, CHEN Zhi-gang. Preparation and catalytic properties of $Ce_{1-x}Mn_xO_{2-\delta}$−attapulgite nanocomposite materials [J]. The Chinese Journal of Nonferrous Metals, 2011, 21(7): 1580−1586. (in Chinese)

[20] HU K H, LIU Z, HUANG F, HU X G, HAN C L. Synthesis and photocatalytic properties of nano-MoS_2/kaolin composite [J]. Chem Eng J, 2010, 162: 836−843.

[21] HU K H, CAI Y K, SHAO G Q, CUI X L. Synthesis and photocatalytic properties of nano-MoS_2/AlOOH composite [J]. React Kinet Mech Catal, 2011, 103: 153−164.

[22] JIA Zhi-gang, PENG Kuan-kuan, LI Yan-hua, ZHU Rong-sun. Preparation and photocatalytic performance of porous ZnO microrods loaded with Ag [J]. Transactions of Nonferrous Metals Society of China, 2012, 22(4): 873−878.

[23] ŞOLPAN D, DURAN S, SARAYDIN D, GÜVEN O. Adsorption of methyl violet in aqueous solutions by poly(acrylamide-co-acrylic acid) hydrogels [J]. Radiat Phys Chem, 2003, 66: 117−127.

[24] HO Y S. Second-order kinetic model for the sorption of cadmium onto tree fern: A comparison of linear and non-linear methods [J]. Water Res, 2006, 40: 119−125.

纳米 MoS_2/膨润土复合物的合成及其在去除有机染料中的应用

胡坤宏[1,2], 赵娣芳[1], 刘俊生[1]

1. 合肥学院 化学与材料工程系，合肥 230022；
2. 合肥工业大学 材料科学与工程博士后科研流动站，合肥 230009

摘　要：通过在 H_2 中煅烧沉积在膨润土表面的 MoS_3，制备纳米 MoS_2/膨润土复合物。利用热重分析、X 射线衍射、扫描电镜和透射电镜等对获得的复合物进行表征。结果表明：纳米 MoS_2 微粒分布在膨润土表面并形成层状结构，层间距大约为 0.64 nm。获得的复合物具有优良的脱除甲基橙的性能，并受到复合物用量、甲基橙初始浓度、温度和 pH 值等操作条件的影响，但不受光源的影响。复合物脱除甲基橙属于吸附机理，符合准二级动力学模型。

关键词：二硫化钼；膨润土；纳米微粒；光催化；吸附；有机染料

(Edited by FANG Jing-hua)